Eur. Phys. J. D **45**, 247–252 (2007)
DOI: 10.1140/epjd/e2007-00267-5

THE EUROPEAN PHYSICAL JOURNAL D

The hydrogenated aluminium trimer: a theoretical examination of the formation and interconversion pathways*

J. Moc[a]

Faculty of Chemistry, Wroclaw University, F. Joliot-Curie 14, 50-383 Wroclaw, Poland

Received 15 May 2007 / Received in final form 6 August 2007
Published online 21 September 2007 –

Abstract. Five doublet isomers of the Al_3H_2 cluster lying within a narrow range of 5 kcal/mol, along with the isomerization transition states connecting them, have been located with the coupled-cluster CCSD(T) and DFT methods. The two most stable doublet structures, the C_{2v} planar including the two Hs bound terminally and C_1 non-planar showing one H in terminal site and the other in threefold site are found to be essentially degenerate. Although the reaction of Al_3 with H_2 to yield Al_3H_2 is found to be significantly exothermic, by 23.5 kcal/mol, this hydrogenation is impeded by a considerable kinetic barrier of 16 kcal/mol. Our result is consistent with the observed lack of reactivity of Al_n towards $H_2(D_2)$ for $n = 3$ under thermal conditions [3]. The quartet Al_3H_2 isomers are predicted to lie 16–21 kcal/mol higher in energy than the doublet analogues. Further dimerization of Al_3H_2 to form Al_6H_4 has also been examined.

PACS. 31.15.Ar Ab initio calculations – 31.15.Ew Density-functional theory – 36.40.-c Atomic and molecular clusters – 36.40.Jn Reactivity of clusters

1 Introduction

There are many examples in the literature demonstrating a strong size-dependence of the reactivity of small main group and transition metal clusters (see, e.g., Refs. [1–3]). For aluminium, this was confirmed by a study of Cox et al. [3] on the reactions of the gas phase Al_n clusters ($n \leqslant 30$) with several simple molecules including H_2 and D_2. Employing the pulsed cluster beam flow reactor technique combined with photoionization time-of-flight mass spectrometry, these authors measured the reactivity of Al_n clusters towards $H_2(D_2)$ under thermal conditions. With the use of the "small diameter reactor", Cox et al. indicated for the latter processes an oscillatory behaviour in the relative rate constant between $n = 2$ and $n = 8$, i.e., with the alternating minima and maxima for odd and even n, respectively. The complementary infrared (IR) matrix isolation experiments by Andrews group [4] on the reactivity of small Al_n clusters with H_2 dealt with those having $n = 1$, 2. For the reaction of Al atom with H_2 to yield AlH and AlH_2 hydrides, activation either by photolysis or by excess energy from the ablation process was required [4]. By contrast, the hydrogenation of aluminium dimer to form Al_2H_2 hydride was found to take place spontaneously in a noble gas matrix [4]. Previously, we compared the performance of highly correlated single- and multi-reference ab initio and density functional methods to study the reaction $Al_2 + H_2$ to form Al_2H_2 [5]. In addition to the high exothermicity of this hydrogenation reaction of ca. 39 kcal/mol relative to the ground state $Al_2(^3\Pi_u) + H_2$ reactants, no activation barrier was found on the singlet potential energy surface (PES), consistent with the matrix isolation results [4].

The calculations presented here extend the earlier work on the reactivity of the small Al_n clusters towards molecular hydrogen to $n = 3$. In the gas phase pulsed cluster beam/mass spectrometry study of the Al_n+$H_2(D_2)$ systems, for Al_3 ($n = 3$), the lack of reactivity was observed under thermal conditions [3]. Due to the presence of low-lying doublet and quartet states for the bare Al_3 cluster, an issue discussed in detail below, both the lowest doublet and quartet PES of Al_3H_2 have been explored. Further dimerization of Al_3H_2 to form Al_6H_4 has been also studied.

2 Computational methods

The aug-cc-pVTZ basis set [6] was used. The lowest doublet and quartet potential energy surfaces of Al_3H_2 were explored with density functional theory (DFT) employing the hybrid B3LYP functional [7,8]. Optimized structures were calculated together with the force constant matrices (Hessians) to provide harmonic vibrational frequencies and zero-point energy (ZPE) values, included in the quoted relative energies. Minima on the PES were

* Table S.1 collecting the calculated IR spectra of the Al_3H_2 isomers is only available in electronic form at `www.epj.org`

[a] e-mail: `jmoc@wchuwr.chem.uni.wroc.pl`

Table 1. Energies (kcal/mol) of the Al_3 stable structures[a].

	B3LYP[b]		CCSD(T)[b]		Previous calcs.
	ΔE	ΔE^c	ΔE	ΔE^c	
$Al_3(D_{3h}, {}^2A_1')$	0.0	0.0	0.0	0.0	0.2[d], 0.2[e], 0.0[f], 0.0[g], 0.0[0.0][h]
$Al_3(C_{2v}, {}^4A_2)$	3.3	3.1	5.2	5.1	0.0[d], 0.0[e], 2.3[f], 4.6[g], 4.9[5.5][h]
$Al_3(D_{3h}, {}^2A_2'')$	4.3	4.1	4.2	3.9	2.8[d], 7.4[f], 5.9[g], 4.4[5.0][h]
$Al_3(D_{\infty h}, {}^2\Pi_u)$	16.2	15.8	21.6	21.3	14.1[d], 21.7[g]

[a]For the geometrical parameters, see Figure 1. [b]At the B3LYP geometries. [c]Corrected for the differences in unscaled B3LYP ZPEs. [d]MRCI/ECP, r(Al-Al) = 2.59 Å ($^2A_1'$), 2.62 Å ($^4A_2$), 2.86 Å ($^2A_2''$), 2.78 Å ($^2\Pi_u$), reference [12]. [e]MRCI/ECP, r(Al-Al) = 2.59 Å ($^2A_1'$), 2.62 Å ($^4A_2$), reference [13]. [f]DFT/ECP, r(Al-Al) = 2.46 Å ($^2A_1'$), 2.55 Å ($^4A_2$), 2.56 Å ($^2A_2''$), reference [16]. [g]DFT BP86, r(Al-Al) = 2.52 Å ($^2A_1'$), 2.60 Å ($^4A_2$), 2.62 Å ($^2A_2''$), 2.80 Å ($^2\Pi_u$), reference [17]. [h]CCSD(T)[CCSDT], r(Al-Al) = 2.541 Å ($^2A_1'$), 2.599 Å ($^4A_2$), 2.632 Å ($^2A_2''$), reference [14]. The other CCSD(T) calculations (Ref. [15]) provided the following relative energies (kcal/mol): 0.0 ($^2A_1'$), 6.6 ($^4A_2$), 5.1 ($^2A_2''$) and bond lengths (Å) 2.544 ($^2A_1'$), 2.603 ($^4A_2$), 2.636 ($^2A_2''$) (for the $^4A_2$ state, the shorter Al-Al distance is given).

connected to each transition state (TS) by tracing the intrinsic reaction coordinate (IRC) [9]. The relative energies, especially the barrier heights, were also calculated using ab initio singles and doubles coupled-cluster method with perturbative triples (CCSD(T)) [10] assuming the DFT structures. It was shown previously for Al_2H_2 [5] that the CCSD(T)//DFT computational level performed well compared to the more sophisticated CCSD(T)//CCSD and SOCI/CASSCF ab initio schemes. Based on these earlier results, the CCSD(T)//DFT level is expected to be adequate for the larger Al_3H_2 system. The calculations were carried out with Gaussian 03 [11].

3 Results and discussion

3.1 Bare Al_3 cluster

The bare aluminium trimer was investigated before employing multi-reference configuration interaction (MRCI) [12,13], single-reference CCSD(T) [14,15] and density functional [15–17] methods. Using different variants of MRCI in conjunction with the effective core potential (ECP) for Al, Petersson et al. [12] and Meier et al. [13] predicted the triangular quartet $^4A_2$ electronic ground state in C_{2v} symmetry to be 0.2 kcal/mol lower in energy than the triangular doublet $^2A_1'$ state in D_{3h} symmetry. The subsequent DFT studies by Jones [16] and Ahlrichs and Elliott [17] indicated the doublet $^2A_1'(D_{3h})$ ground state. Extensive examination of the low-lying electronic states of Al_3 by using coupled-cluster (CC) theory was conducted by Baeck and Bartlett [14] who calculated the geometries and energetic splittings employing both the CCSD(T) and CCSDT variants. The doublet $^2A_1'(D_{3h})$ ground state was found again at both the CCSD(T) and CCSDT (at the CCSD(T) geometries) computational levels, with the doublet $^2A_2''(D_{3h})$ state and quartet $^4A_2(C_{2v})$ and $^4B_1(C_{2v})$ states located 4.4 (5.0), 4.9 (5.5) and 5.9 (6.5) kcal/mol above the ground state, respectively, with CCSD(T) (CCSDT) [14] (for the summary of the previous calculations on Al_3, cf. Tab. 1).

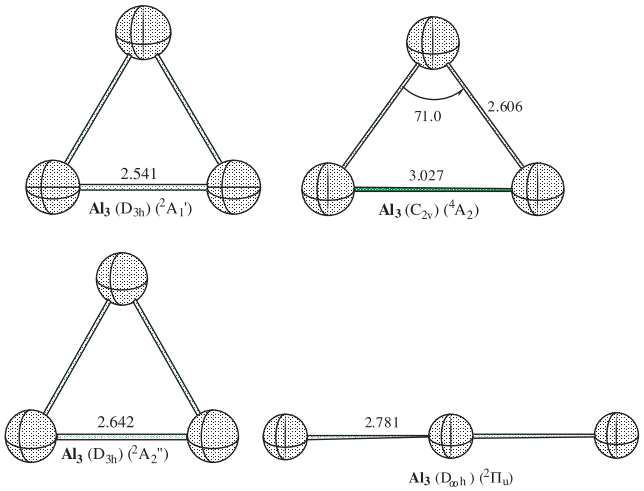

Fig. 1. Optimized equilateral triangular (D_{3h}, $^2A_1'$, $^2A_2''$), isosceles triangular (C_{2v}, $^4A_2$) and linear ($D_{\infty h}$, $^2\Pi$) structures of bare Al_3 cluster (bond lengths in Å, bond angles in degrees).

Our both B3LYP and CCSD(T) results indicate that the ground state of Al_3 is the $^2A_1'$ state in D_{3h} symmetry (Fig. 1, Tab. 1), in keeping with the most recent DFT and coupled-cluster results [14–17]. Similarly, the equilateral triangular doublet $^2A_2''$ and isosceles triangular quartet $^4A_2$ are found to be the low-lying states of Al_3, consistent with the previous reports [12–17]. Especially, our CCSD(T) state order and corresponding energetic separations in Table 1 compare favourably with the earlier coupled-cluster results [14,15]. Likewise, our calculated Al-Al distances of 2.541 Å ($^2A_1'$), 2.642 Å ($^2A_2''$) and of 2.606 and 3.027 Å ($^4A_2$) along with the bond angle of 71.0° for the latter state (Fig. 1) are in excellent agreement with the reported DFT and CCSD(T) parameters [14,15]. The Al_3 doublet ground state was also inferred from both the magnetic deflection [18] and noble gas matrix isolation electron spin resonance (ESR) [19] experiments (the early ESR study in hydrocarbon matrix indicated a quartet ground state [20]). On the other hand, the triangular

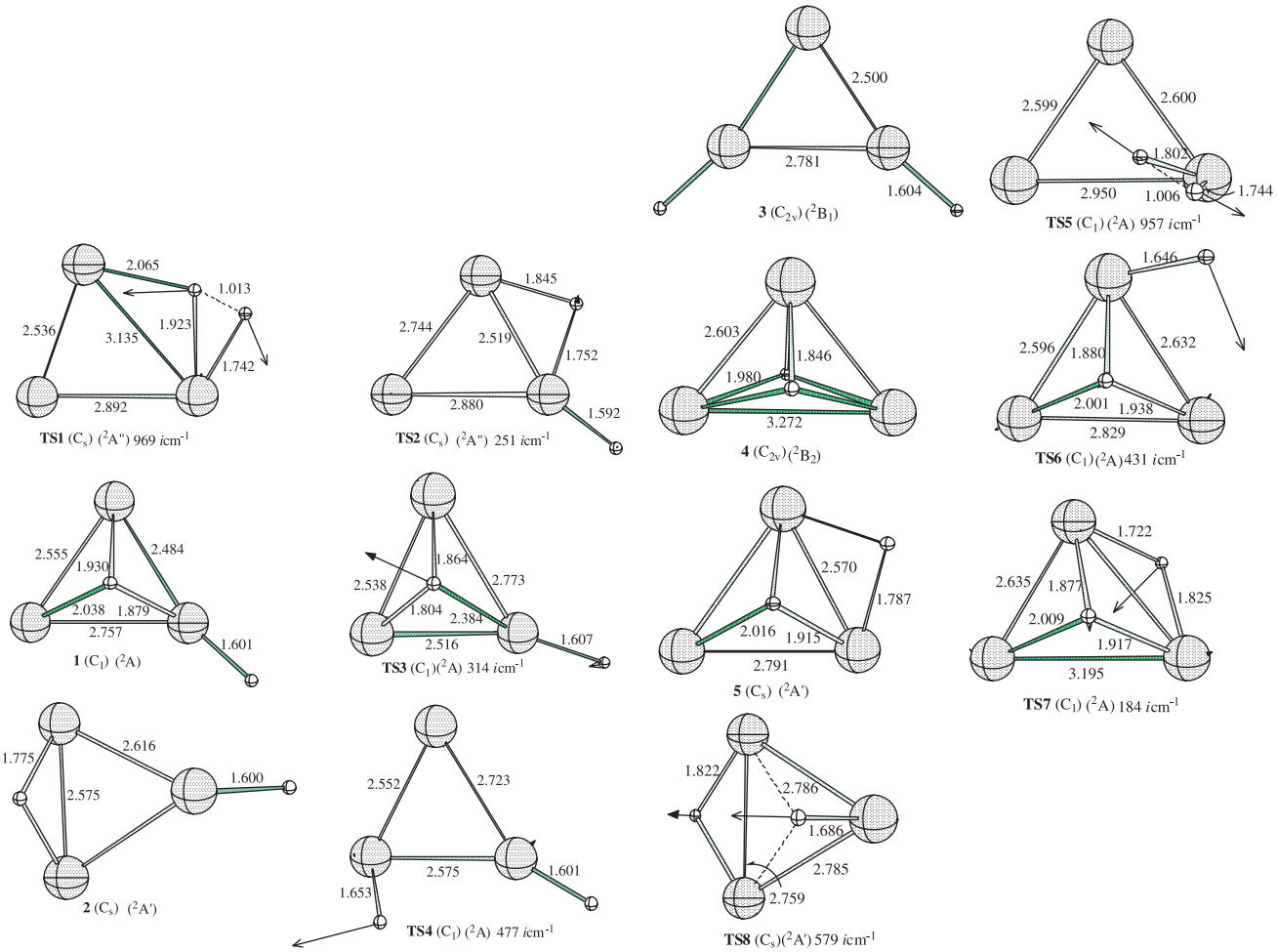

Fig. 2. Al_3H_2 doublet minimum and transition state (TS) structures (bond lengths in Å). The reaction coordinate vector and corresponding imaginary frequency is shown for each TS.

$^4B_1$ state appeared to be associated with the structure unstable relative to b_2 (249 $i$cm^{-1}) vibrational mode. According to Table 1, the lowest linear $^2\Pi$ state is not energetically competitive with the triangular-like states, in line with the previous calculations [12,13,16,17]. In view of the above results, in the present study we have considered hydrogenation reaction of the triangular Al_3 to form Al_3H_2 cluster along with the rearrangements of the latter.

3.2 Hydrogenation of Al_3 and isomerization of Al_3H_2

The doublet minima and transition state (TS) structures engaged in the formation and isomerization of the Al_3H_2 cluster are shown in Figure 2, with the appropriate quartet structures drawn in Figure 3. The summarizing CCSD(T)//B3LYP energy diagram for the reactions studied, based on the relative energies in Table 2, is depicted in Figure 4. The lower energy doublet paths are reported first, and unless otherwise stated, the values quoted hereafter refer to the ZPE corrected CCSD(T)//B3LYP [21] results.

The planar transition state for the H-H bond breakage located on the $^2A''$ PES, **TS1**(^{2}**A**$''$), features the H-H distance of 1.013 Å and ultimate weakening of the Al-Al bond (of 3.13 Å) adjacent to the H-H bond breaking (Fig. 2). The resulting $Al_3H_2(^2A'')$ activation "product" obtained by following the IRC from **TS1** appears to be a saddle point itself, **TS2**(^{2}**A**$''$), for interconversion of the equivalent non-planar Al_3H_2 minima **1**(^{2}**A**). Thus, the bifurcation of the $^2A''$ PES occurs in this region. If one follows the degenerate path **1**(^{2}**A**) → **TS2**(^{2}**A**$''$) → **1**(^{2}**A**), the threefold bonded H atom is displaced from one side of the Al_3 plane to the other.

The isomer **1** can be reached directly by proceeding the C_1 path via transition state **TS5**(^{2}**A**) for H-H activation (Fig. 4). The IRC calculation confirmed that **TS5** connects with the Al_3H_2 isomer **1**. The H-H bond breaking at the **TS5** structure, with r(H-H) = 1.006 Å, is accompanied again by a considerable elongation of one of Al-Al bonds (with r(Al-Al) = 2.95 Å) (Fig. 2). Importantly, the C_1 path requires traversing a barrier of 16.3 kcal/mol relative to $Al_3(^2A_1')$ + H_2. The doublet structure **1**, lying 23.5 kcal/mol below the ground-state reference, is found to be the most stable isomer of the Al_3H_2 cluster (see, however, below for the other close lying doublet isomers). In addition to one H in threefold position (Al-H = 1.88,

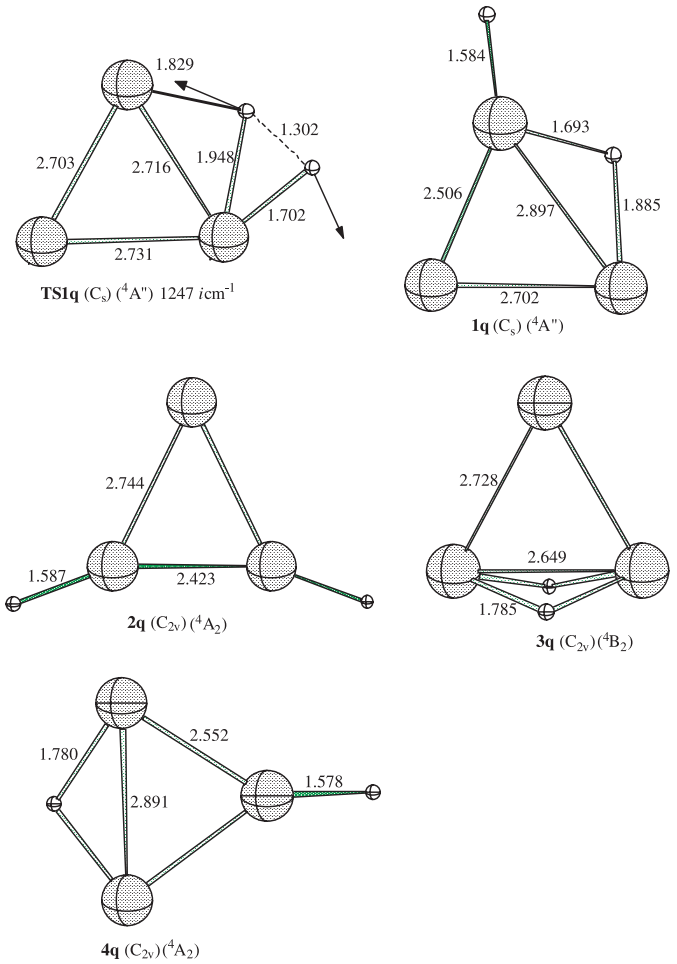

Fig. 3. Al_3H_2 quartet minimum and transition state (TS) structures. Conventions as in Figure 2.

1.93, 2.04 Å), **1** exhibits the other H in terminal position (Al-H = 1.60 Å). The hydrogen shift from the threefold site of **1** to the bridged site via transition state **TS3**, leading to the C_s isomer **2**(^{2}**A′**), is a facile rearrangement, with an associated barrier of only 1.6 kcal/mol. However, the barrier height for the reverse process (**2** → **1**) amounting only to 0.6 kcal/mol does not assure a kinetic stability of **2**. The alternative H migration from the threefold site of **1** taking place to the terminal site via transition state **TS4** gives rise to the C_{2v} planar isomer **3**(^{2}**B**$_1$) having two terminal Al-H bonds of 1.60 Å. During this rearrangement the binding of H to two Al atoms is lost and, consequently, it requires overcoming a relatively high barrier of 11.2 kcal/mol. The planar Al_3H_2 isomer **3** is located 23.3 kcal/mol below $Al_3(^2A_1') + H_2$ and is indicated to be nearly degenerate with **1** (Tab. 2, Fig. 4).

The different kind of rearrangement of cluster **1**(^{2}**A**) occurs, when a rotation of the terminal Al-H bond takes place via transition state **TS6** (Fig. 2). The emerging C_s isomer **5**(^{2}**A′**), holding the Hs in threefold and bridge sites, lies 18.6 kcal/mol below $Al_3(^2A_1') + H_2$ and it is the least stable among the doublet Al_3H_2 species. However, further movement of the bridged hydrogen in **5** to the threefold site through transition state **TS7** leads to a more stable Al_3H_2 isomer **4**(^{2}**B**$_2$) of C_{2v} symmetry. The latter species thus exhibits both Hs in two equivalent threefold positions, and this particular arrangement leads to a substantial lengthening of one of the Al-Al bonds of **4** to 3.27 Å (Fig. 2). The isomer **4** is stabilized by 22.4 kcal/mol with respect to $Al_3(^2A_1') + H_2$, being essentially degenerate with **2** and only 1 kcal/mol less favourable than the most stable Al_3H_2 species **1** and **3**. On the other hand, the **2** → **5** isomerization involves inversion of the terminal H via **TS8** (^{2}**A′**) to reach the threefold site. As expected, this is the most energetically demanding rearrangement on the doublet PES studied here, with **TS8** lying 20 kcal/mol above **2** (Fig. 4).

Table 2. Energies (kcal/mol) of the species along the calculated $Al_3 + H_2 \rightarrow Al_3H_2$ reaction paths.

	B3LYP[a]		CCSD(T)[a]	
	ΔE	ΔE^b	ΔE	ΔE^b
$Al_3(^2A_1') + H_2$	0.0	0.0	0.0	0.0
TS1(^{2}A″)	16.5	15.5	20.3	19.3
TS2(^{2}A″)	–20.2	–19.7	–18.2	–17.7
1(^{2}A)	–25.4	–24.6	–24.3	–23.5
TS3(^{2}A)	–23.6	–23.1	–22.5	–21.9
2(^{2}A′)	–25.0	–23.8	–23.7	–22.5
TS4(^{2}A)	–14.6	–14.6	–12.3	–12.3
3(^{2}B$_1$)	–25.5	–24.6	–24.2	–23.3
TS5(^{2}A)	13.4	13.1	16.5	16.3
4(^{2}B$_2$)	–25.9	–24.7	–23.6	–22.4
TS6(^{2}A)	–16.6	–16.4	–14.3	–14.1
5(^{2}A′)	–21.4	–20.5	–19.5	–18.6
TS7(^{2}A)	–17.9	–17.4	–14.7	–14.2
TS8(^{2}A)	–6.6	–7.5	–1.7	–2.6
$Al_3(^4A_2) + H_2$	3.3	3.1	5.2	5.1
TS1q (^{4}A″)	24.7	23.7	27.3	26.3
1q (^{4}A″)	–9.1	–7.6	–8.4	–6.9
2q (^{4}A$_2$)	–7.9	–6.8	–6.8	–5.6
3q (^{4}B$_2$)	–4.1	–2.6	–2.9	–1.4
4q (^{4}A$_2$)	–8.9	–7.6	–7.8	–6.5

[a] At the B3LYP geometries. [b] Corrected for the differences in unscaled B3LYP ZPEs.

On the quartet PES, the C_s hydrogenation path leading to the **1q**(^{4}**A″**) isomer of Al_3H_2 has been located (note that the doublet analogue of **1q** corresponds to an unstable saddle point). This path involves "late" transition state for H-H bond breakage **TS1q**(^{4}**A″**) with r(H-H) = 1.30 Å and is associated with a sizable barrier of 26.3 (21.2) kcal/mol relative to the $Al_3(^2A_1') + H_2$ ($Al_3(^4A_2) + H_2$) asymptote (Figs. 3 and 4). The confirmed by the IRC calculation quartet Al_3H_2 product, **1q**(^{4}**A″**), contains one H bound terminally (Al-H = 1.58 Å) and the other H in bridge position (Al-H = 1.69, 1.88 Å). It is interesting to note that similar to the doublet Al_3H_2 species, **1q** is also predicted to lie below the ground-state asymptote, i.e., by 6.9 kcal/mol. The additional three Al_3H_2 quartet minima **2q**(^{4}**A**$_2$), **3q**(^{4}**B**$_2$) and **4q**(^{4}**A**$_2$) (Fig. 3) have been identified and also found to lie below the ground-state asymptote, by 5.6, 1.4 and 6.5 kcal/mol, respectively (Tab. 2, Fig. 4). We have not pursued, however,

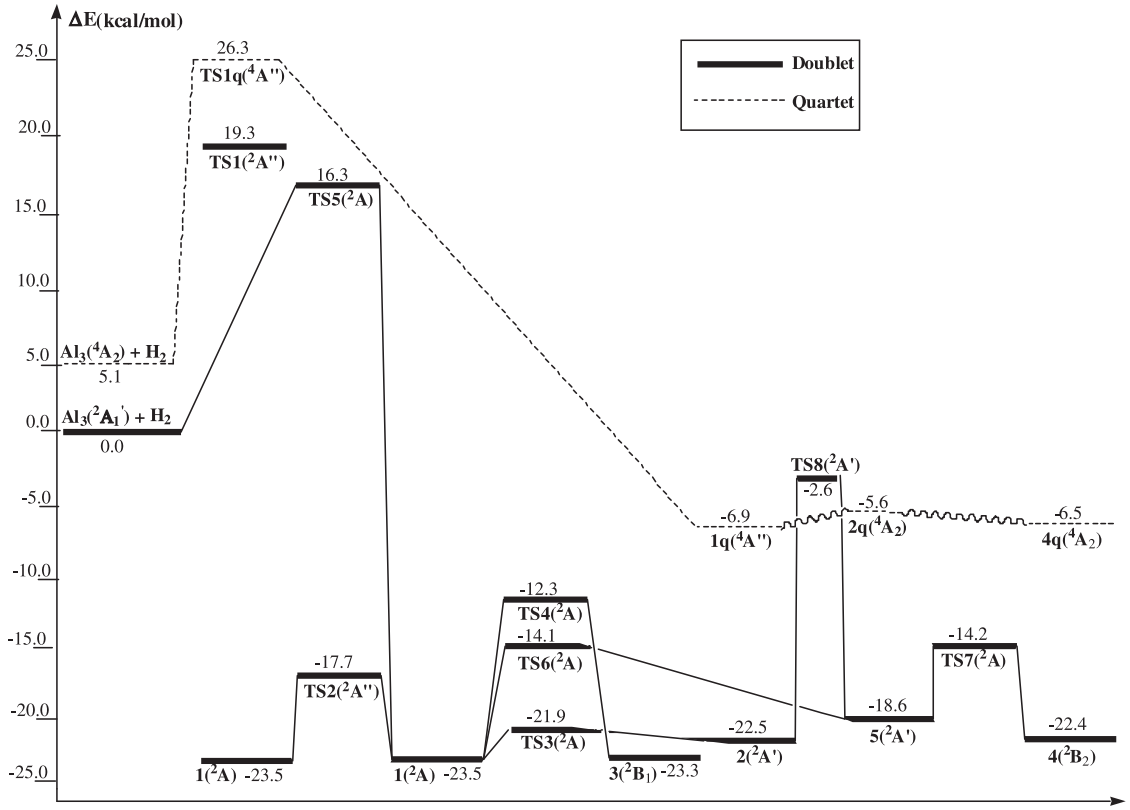

Fig. 4. CCSD(T)//B3LYP + ZPE potential energy profile of Al_3H_2. All energies (kcal/mol) are given with respect to the $Al_3(^2A_1')$ + H_2 ground-state reference.

the isomerization paths of these less stable (compared to the doublet species) quartet clusters. To the best of our knowledge, the only previous theoretical study on the hydrogenation of Al_3 is that by Kawamura et al. [22]. Using a density functional method with ultrasoft pseudopotentials and plane-wave basis set these authors looked at atomic and molecular hydrogenation of Al_3 by studying structures, stabilities and bonding nature of the Al_3H and Al_3H_2 clusters. In the latter case only doublet structures were calculated. However, those which we have found here as the most stable ones (**1**,**3**) were not considered in reference [22]. Also, neither the $Al_3 + H_2 \rightarrow Al_3H_2$ reaction path nor kinetic stability of the Al_3H_2 species were previously discussed.

In summary, the highly exothermic reaction between Al_3 and H_2 to form the doublet Al_3H_2 species (by 23.5 kcal/mol) is predicted to be inhibited by a significant barrier height of 16.3 kcal/mol. This finding is consistent with the experimental observation: the reaction $Al_n + H_2 \rightarrow Al_nH_2$ did not take place for $n = 3$ under thermal conditions [3]. Five doublet and four quartet isomers of the Al_3H_2 cluster have been identified along with the interconversion TSs (doublet case), all the species lying below the asymptote $Al_3(^2A_1') + H_2$.

3.3 Dimerization of Al_3H_2

Associated with an Al_3H_2 species (assuming its successful formation) is the possible dimerization to yield a larger cluster Al_6H_4. The calculated structures and relative stabilities of the latter are shown in Figure 5 and Table 3, respectively (the ZPE corrected B3LYP results). The four Al_6H_4 structures found, named **Al6H4_1**, **Al6H4_2**, **Al6H4_3** and **Al6H4_4** possess C_{2h}, C_1, C_1 and C_s symmetries, respectively. They have similar relative energies, lying within 5.6 kcal/mol. The first three clusters derive from a distorted octahedral Al_6 core, while this core is of capped tetragonal pyramid kind in the case of the last Al_6H_4 cluster. It can be noted here that the **Al6H4_1** structure showing the four Hs positioned on the single (terminal) Al atoms resembles that reported for Al_6H_4 by Kawamura et al. [23]. It is seen further from Table 3 that the **Al6H4_2** and **Al6H4_3** clusters are nearly degenerate, which can be readily explained by their structural resemblance. The important finding here is a large exothermicity of the reaction $2Al_3H_2 \rightarrow Al_6H_4$ of 62.7 kcal/mol (Tab. 3), indicating that the process is likely to be barrier free.

4 Conclusions

For the bare Al_3 cluster, the $^2A_1'(D_{3h})$ electronic ground state is found, in keeping with the most recent DFT and coupled-cluster results [14–17]. Despite a large exothermicity (23.5 kcal/mol), the reaction $Al_3 + H_2 \rightarrow Al_3H_2$ is predicted to have a significant energetic barrier of 16.3 kcal/mol relative to $Al_3(^2A_1') + H_2$. Our finding is

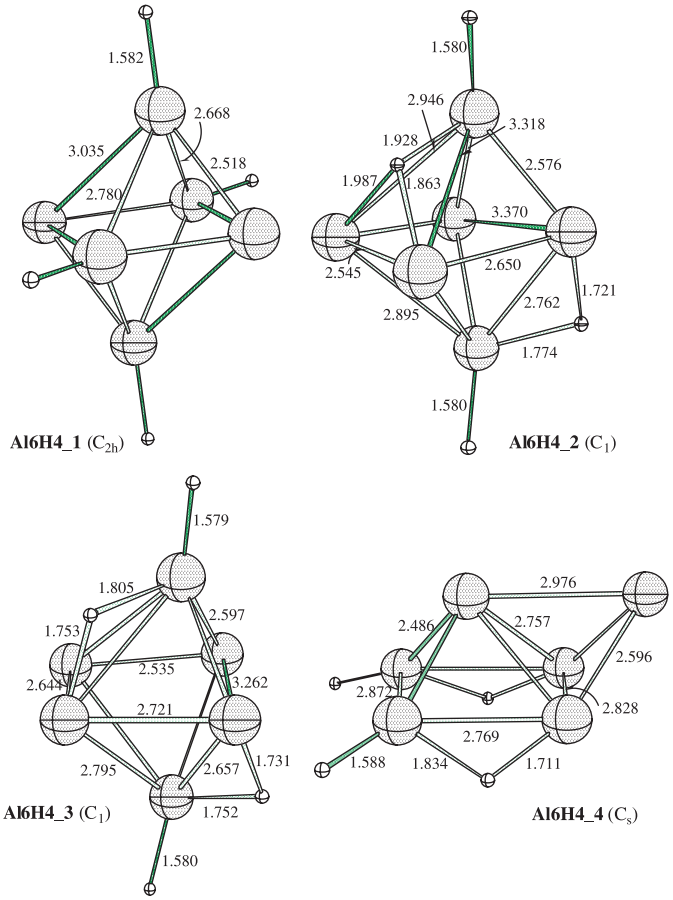

Fig. 5. Al_6H_4 structures (bond lengths in Å).

Table 3. Relative stability of Al_3H_2 isomers[a] and energy of the reaction[b,c] $2Al_3H_2 \rightarrow Al_6H_4$ from the B3LYP calculation (in kcal/mol).

Al_6H_4 cluster[d]	ΔE	ΔE[e]
Al6H4_1(C_{2h}, ^1A_g)	3.4/–61.8	2.9/–59.8
Al6H4_2(C_1, ^1A)	0.1/–65.2	0.0/–62.7
Al6H4_3(C_1, ^1A)	0.0/–65.2	0.2/–62.5
Al6H4_4(C_s, $^1A'$)	5.7/–59.5	5.6/–57.1

[a] Before the slash. [b] After the slash. [c] With respect to two isolated Al_3H_2(**4**, $^2\mathbf{B}_2$) species found to be the lowest energy Al_3H_2 isomer at this computational level (cf. Tab. 2). [d] For the geometrical parameters of **Al6H4_1**, **Al6H4_2**, **Al6H4_3** and **Al6H4_4** clusters see Figure 5. [e] Corrected for the differences in the unscaled B3LYP ZPEs.

consistent with the observed lack of reactivity of Al_n towards $H_2(D_2)$ for $n = 3$ under thermal conditions [3]. The located lowest energy doublet (^{2}A) path is shown to lead directly to the Al_3H_2 cluster most stable isomer **1** (^{2}**A**) having one H in terminal site and the other in threefold site. The nearly degenerate isomer (**3**, $^2\mathbf{B}_1$) is C_{2v} planar with the two Hs bound terminally. In total, five doublet Al_3H_2 minimum structures lying within a narrow interval of 5 kcal/mol has been found, and a detailed study of their interconversion paths is presented. The quartet Al_3H_2 cluster minimum structures are predicted to lie ca. 16–21 (*1.5–7*) kcal/mol above (*below*) the doublet counterparts (*ground-state asymptote*). To guide the future spectroscopic studies of Al_3H_2, the vibrational frequencies and IR intensities for its five doublet isomers have been collected in Table **??**.

The author acknowledges a generous support of computing time at the Wroclaw Center for Networking and Supercomputing.

References

1. P. Fayet, A. Kaldor, D.M. Cox, J. Chem. Phys. **92**, 254 (1990)
2. S. Burkart, N. Blessing, G. Gantefor, Phys. Rev. B **60**, 15639 (1999)
3. D.M. Cox, D.J. Trevor, R.L. Whetten, A. Kaldor, J. Phys. Chem. **92**, 421 (1988)
4. X. Wang, L. Andrews, S. Tam, M.E. DeRose, M.E. Fajardo, J. Am. Chem. Soc. **125**, 9218 (2003) and references cited therein
5. J. Moc, Chem. Phys. Lett. **401**, 497 (2005)
6. T.H. Dunning, J. Chem. Phys. **90**, 1007 (1989)
7. A.D. Becke, J. Chem. Phys. **98**, 5648 (1993)
8. C. Lee, W. Yang, R.G. Parr, Phys. Rev. B **37**, 785 (1988)
9. C. Gonzalez, H.B. Schlegel, J. Chem. Phys. **90**, 2154 (1989)
10. K. Raghavachari, G.W. Trucks, J.A. Pople, M. Head-Gordon, Chem. Phys. Lett. **157**, 479 (1989)
11. M.J. Frisch et al., GAUSSIAN 03, Revision B.05 (Gaussian Inc., Pittsburgh PA, 2003)
12. L.G.M. Petersson, C.W. Bauschlicher, T. Halicioglu, J. Chem. Phys. **87**, 2205 (1987)
13. U. Meier, S.D. Peyerimhoff, F. Grein, Z. Phys. D **17**, 209 (1990)
14. K.K. Baeck, R.J. Bartlett, J. Chem. Phys. **109**, 1334 (1998)
15. C.-G. Zhan, F. Zheng, D.A. Dixon, J. Am. Chem. Soc. **124**, 14795 (2002)
16. R.O. Jones, J. Chem. Phys. **99**, 1194 (1993)
17. R. Ahlrichs, S.D. Elliott, Phys. Chem. Chem. Phys. **1**, 13 (1999)
18. D.M. Cox, D.J. Trevor, R.L. Whetten, E.A. Rohlfing, A. Kaldor, J. Chem. Phys. **84**, 4651 (1986)
19. Y.M. Hamrick, R.J. Van Zee, W. Weltner Jr, J. Chem. Phys. **96**, 1767 (1992)
20. J.A. Howard, R. Sutcliffe, J.S. Tse, H. Dahmane, B. Mile, J. Phys. Chem. **89**, 3595 (1985)
21. P.R. Schreiner, Angew. Chem. Int. Ed. **46**, 4217 (2007)
22. H. Kawamura, V. Kumar, Q. Sun, Y. Kawazoe, Phys. Rev. B **65**, 045406 (2001)
23. H. Kawamura, V. Kumar, Q. Sun, Y. Kawazoe, Phys. Rev. A **67**, 063205 (2003)